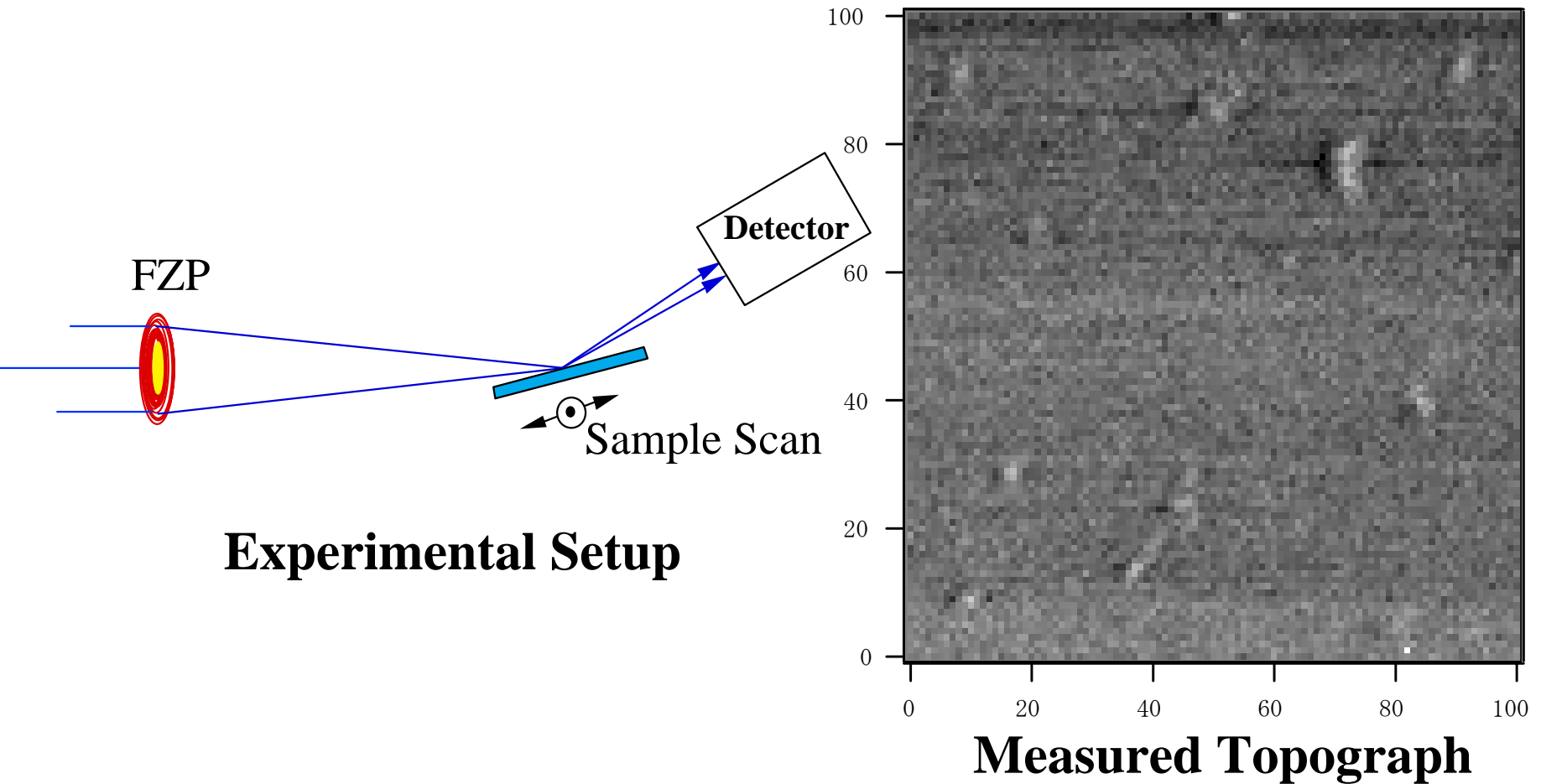


*Emerging Scientific Opportunities with X-Ray Imaging  
at SPring-8*

*Yoshiro Suzuki  
SPring-8, Japan*

2  $\mu\text{m}$

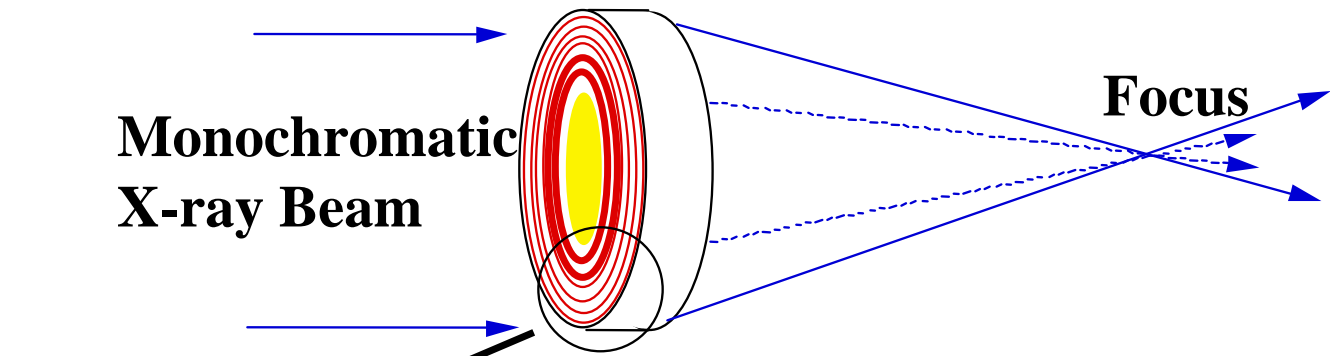


**Experimental Setup**

**Measured Topograph**

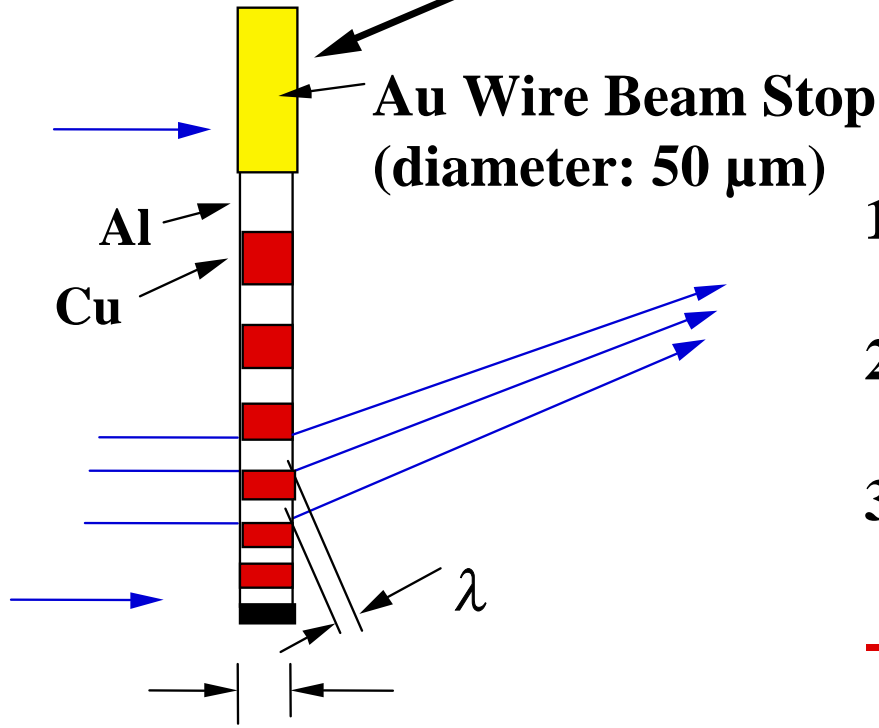
**Si 001 wafer, 9.85 keV, 004 Bragg Reflection,  
101 x 101 pixels, 100 nm x 100 nm pixel, 0.3 s/pixel.**

**Scanning Diffraction-topography  
using Microbeam with 120 nm probe size. @BL20XU**



**Monochromatic  
X-ray Beam**

**Focus**



**Au Wire Beam Stop  
(diameter: 50 μm)**

Al

Cu

$\lambda$

**Thickness: 10 - 40 μm**

### **Advantages of SS-FZP**

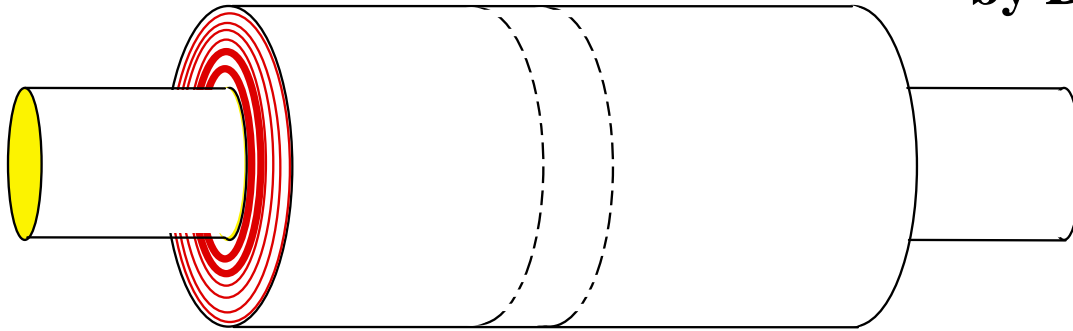
- 1. High Aspect Ratio  
Zone Height/Zone Width > 100.**
  - 2. Narrow Zone Width  
< 100 nm.**
  - 3. Thickness  
No Thickness Limit.**
- > High Energy (~ 100 keV) Optics.**

**Schematic View of Sputtered-sliced Zone Plate**

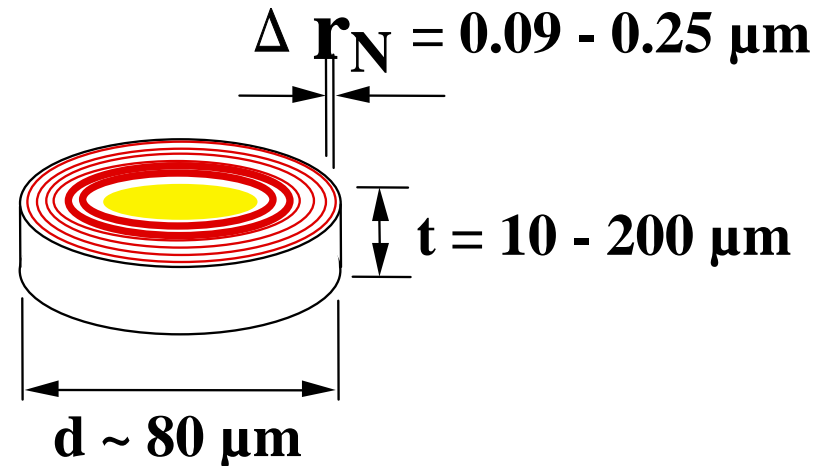
**Gold Wire (Core),  
Diameter  $\sim 50 \mu\text{m}$**



**Multi-layer Coating  
by DC Magnetron Sputtering**

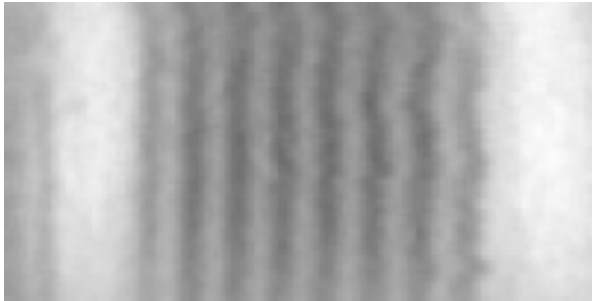


**Cutting and Mechanical Polishing**

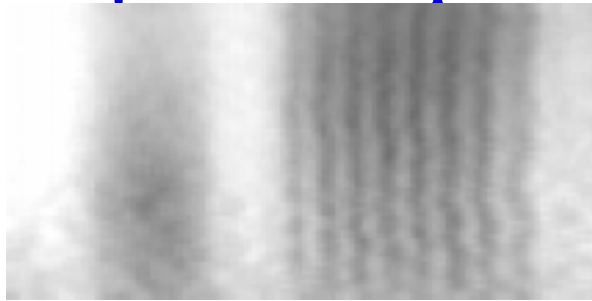


**Fabrication Process of Sputtered-sliced Fresnel Zone Plates**

5  $\mu\text{m}$



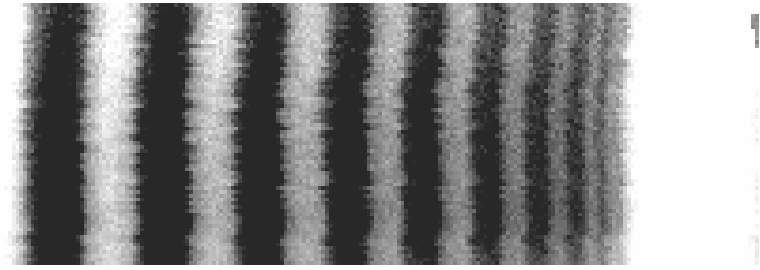
**0.3  $\mu\text{m}$  line & space**



**0.2  $\mu\text{m}$  line & space**

**X-ray wavelength: 1.4  $\text{\AA}$ ,  
128 x 64 pixels,  
0.0625  $\mu\text{m}$ /pixel,  
Dwell time: 0.4s/pixel.**

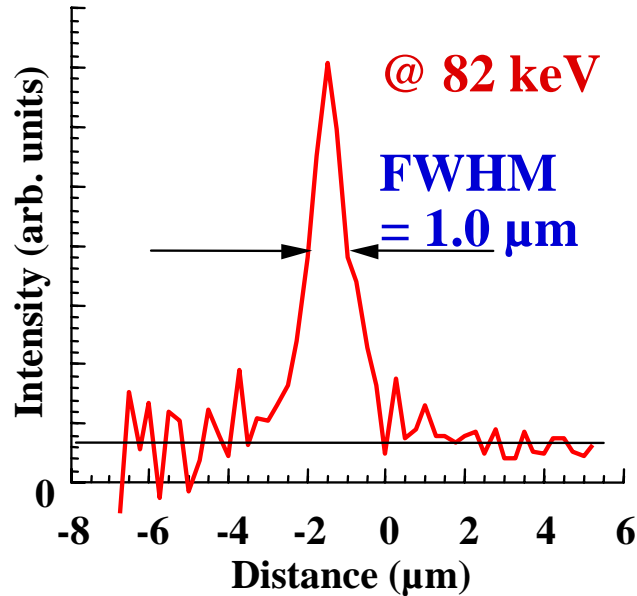
5  $\mu\text{m}$



**0.1  $\mu\text{m}$  line & space**

**X-ray wavelength: 1.0  $\text{\AA}$ ,  
256 x 70 pixel,  
0.0625  $\mu\text{m}$ /pixels,  
Dwell time: 0.4s/pixel.**

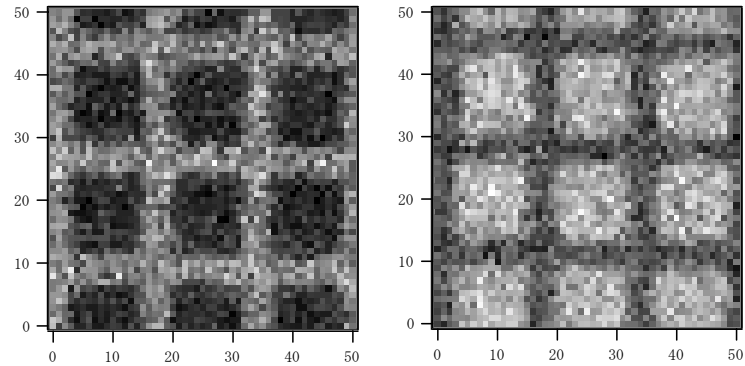
**Scanning Microscopic Image of Resolution Test Pattern**



**Focused Beam Profiles  
measured by Knife-edge Scan**

**X-ray Energy: 82 keV (0.151 Å), f ~ 700 mm,  
Cu/Al sputtered-sliced FZP (50 layers),  
Core (center beam stop): Au 50 μm in diameter,  
Outermost zone width: 0.15 μm,  
Thickness: ~ 40 μm.**

**10 μm**

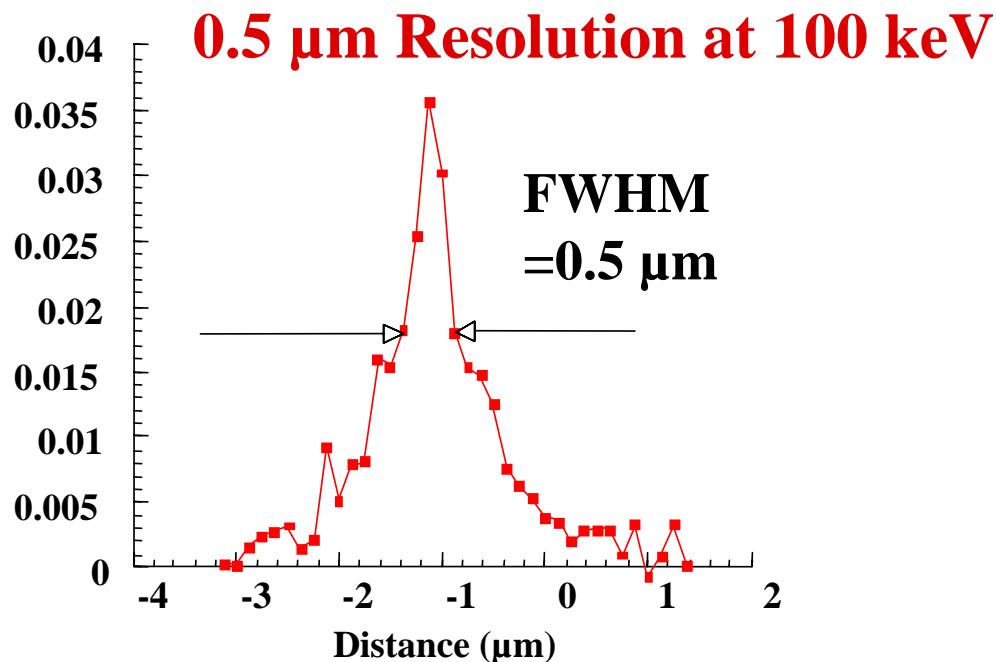


**Scanning Microscopic Image**

**Sample: gold mesh (1500 lines/inch),  
X-ray Energy: 82 keV ,  
51 x 51 pixels,  
1 μm/pixel,  
Dwell time: 2 s/pixel,  
CdZnTe-detector for fluorescent X-rays.**

**Microfocusing/scanning microscopy with SS-FZP at 82 keV**

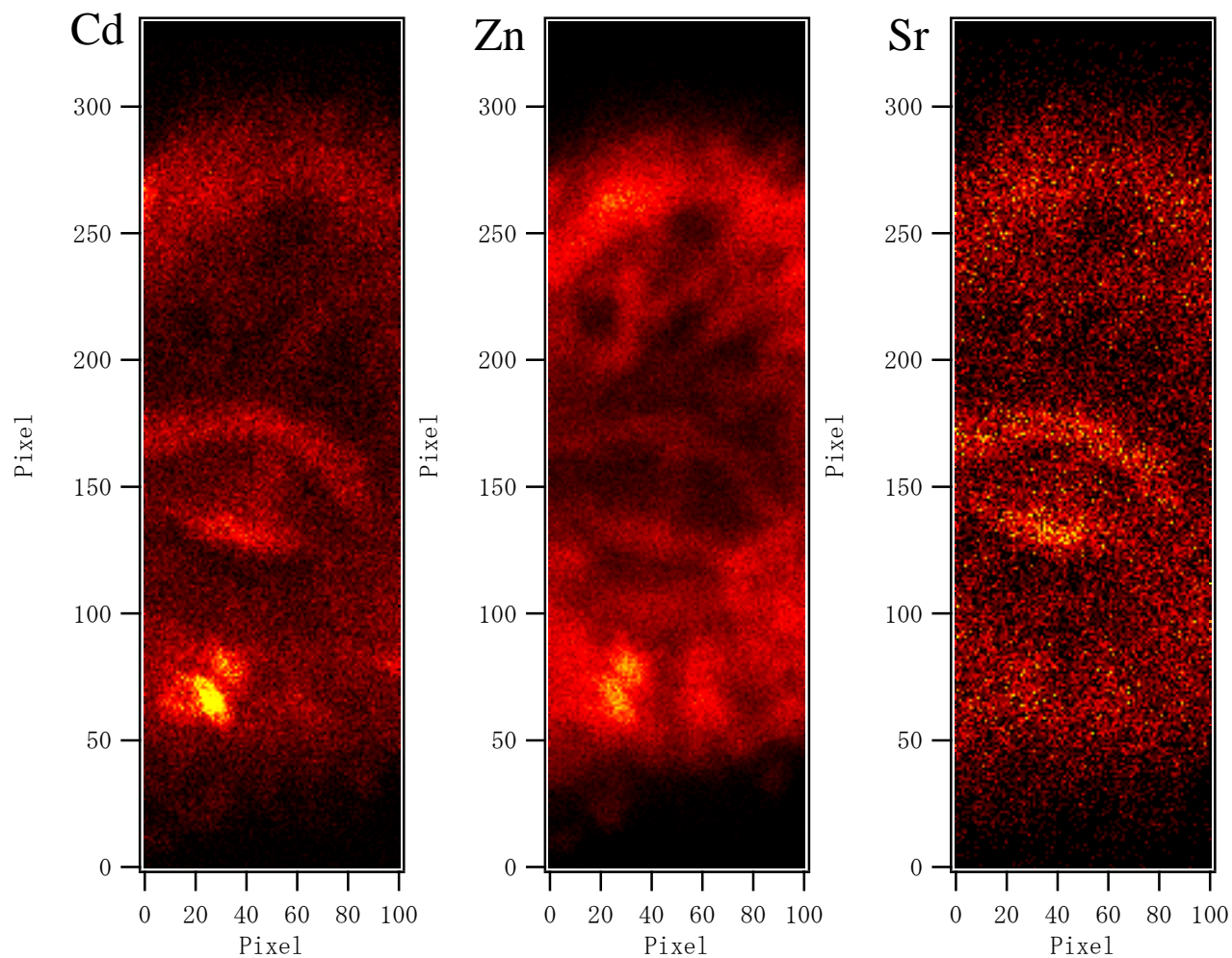
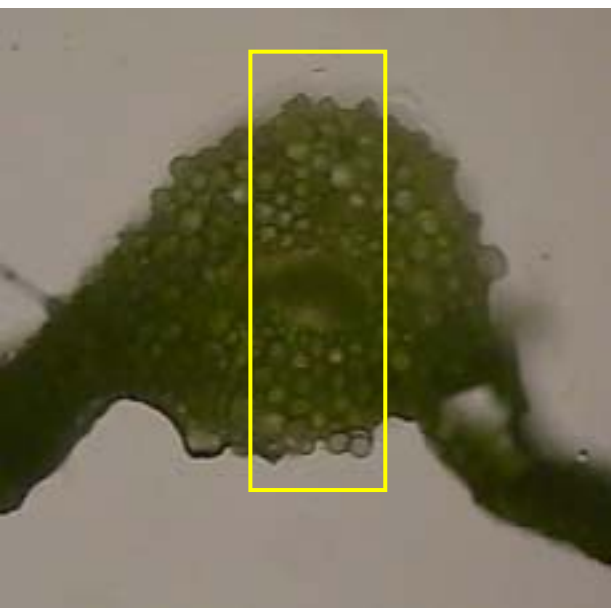
**Diffraction efficiency: 15%**



## **Microbeam with Sputtered-sliced FZP**

**Focused Beam Profile Measured by Edge-scan @BL20XU**

**X-ray wavelength: 0.124  $\text{\AA}$  (100 keV),  $f \sim 900$  mm,  
Cu/Al sputtered-sliced FZP (70 layers),  
Core (beam stop): Au 50  $\mu\text{m}$  in diameter,  
Outermost zone width: 0.16  $\mu\text{m}$ ,  
Thickness:  $\sim 180$   $\mu\text{m}$ .**



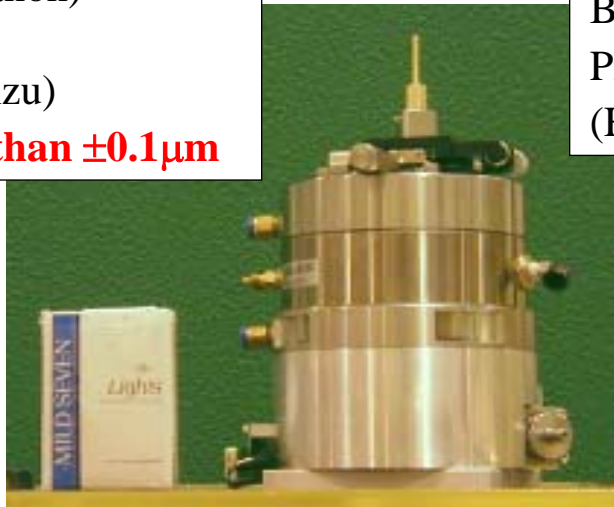
**XRF imaging of a cross section of a leaf which belongs to cruciferous plant.  
Measurement condition: X-ray energy=37 keV, pixel size=3  $\mu\text{m}$  x 3  $\mu\text{m}$ ,  
exposure time=0.2 sec/pixel.**



Air bearing  
AB-80R(Canon)

Rotation stage  
RA-10(Kohzu)

**Wobble is less than  $\pm 0.1\mu\text{m}$**



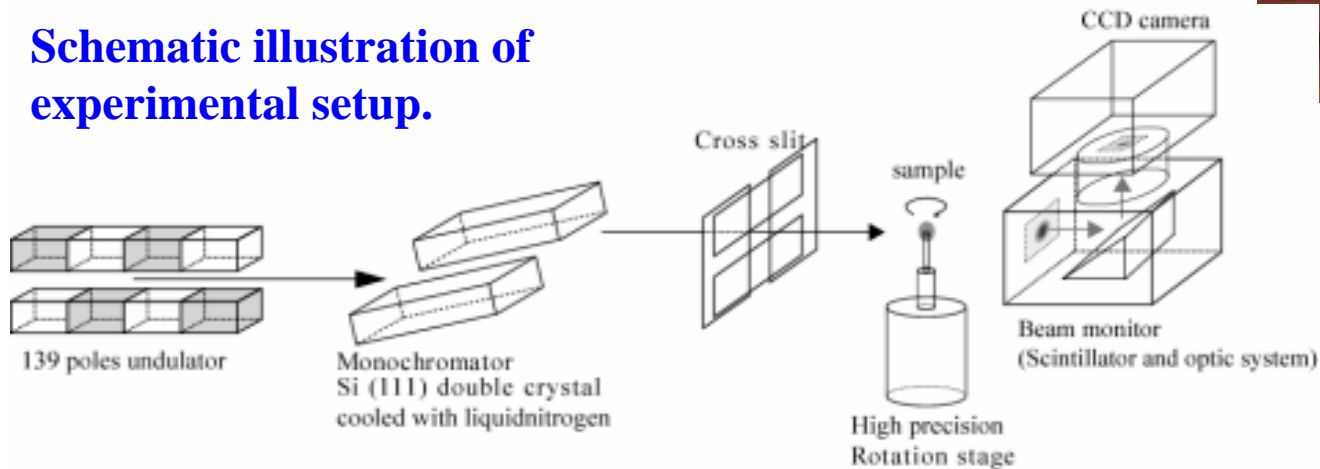
**High precision rotation stage.**

CCD camera: C4880-10-14A  
Beammonitor: AA50(x20, x10)  
Pixel size:  $0.5\mu\text{m}$ ,  $1.0\mu\text{m}$   
(Hamamatsu photonics K.K.)



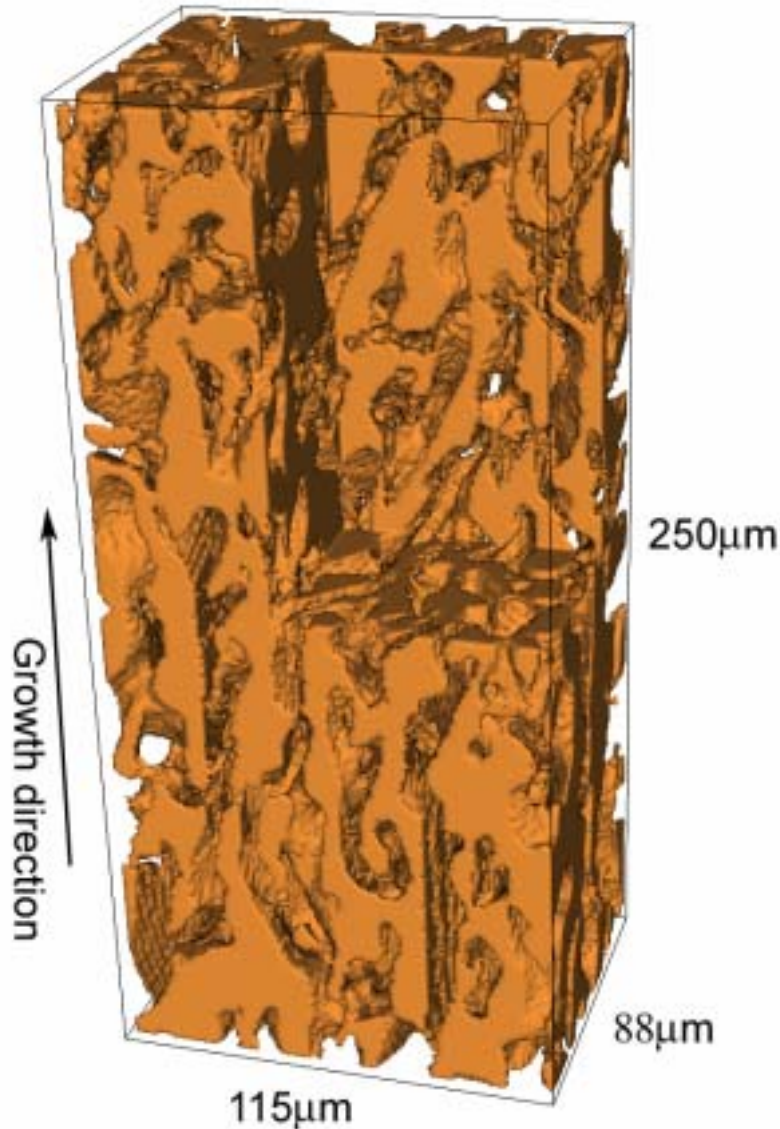
**High resolution detector.**

**Schematic illustration of  
experimental setup.**



**X-ray micro-tomography (3-D imaging with SP- $\mu$ CT 47XU)**

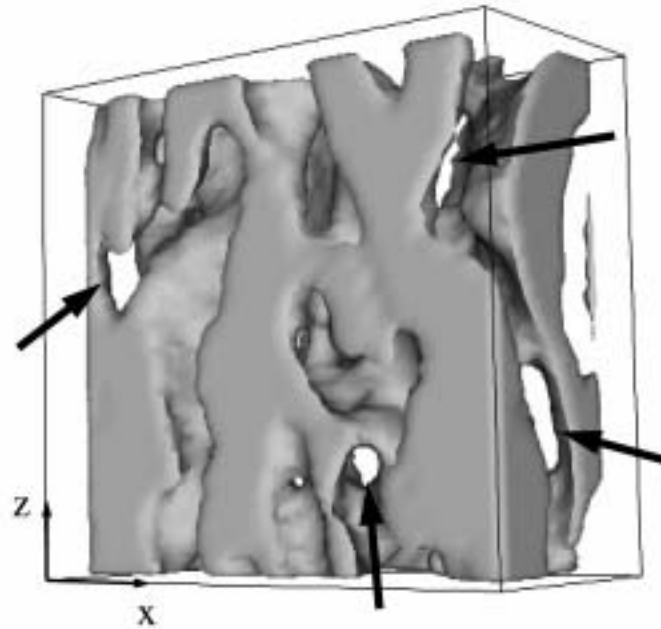
## Investigations of $\text{Al}_2\text{O}_3$ -YAG eutectic structure and their network structure.



Unidirectionally solidified  $\text{Al}_2\text{O}_3$ -based eutectic composites have excellent mechanical properties at high temperatures. For example,  $\text{Al}_2\text{O}_3$ -YAG ( $\text{Y}_3\text{Al}_5\text{O}_{12}$ , yttrium-aluminum-garnet) eutectic composites exhibit excellent mechanical properties from room temperature to 2073K in an air atmosphere and are candidates for high temperature use. The mechanical properties of the above mentioned composites are closely related to their solidified structures. 3D observation shows that the constituent phases with faceted interfaces are three-dimensionally continuous and are complexly entangled with each other. 3D structure obtained by micro X-ray CT allows us to discuss evolution of the eutectic structure during the solidification and origin of the excellent mechanical properties.

**3-D image of  $\text{Al}_2\text{O}_3$ -YAG eutectic structure**

# Network structure in $\text{Al}_2\text{O}_3$ -YAG eutectic composite

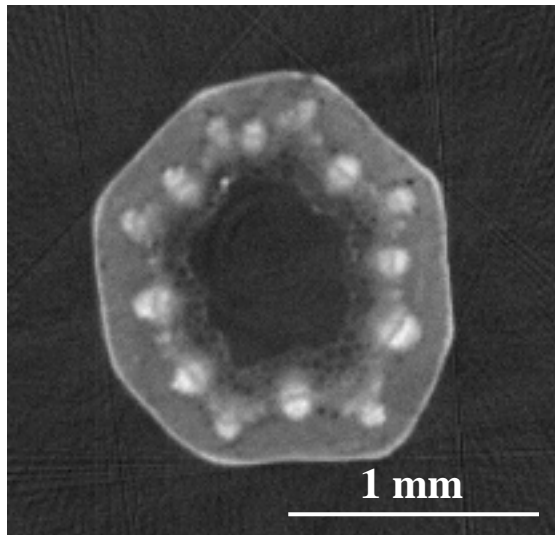
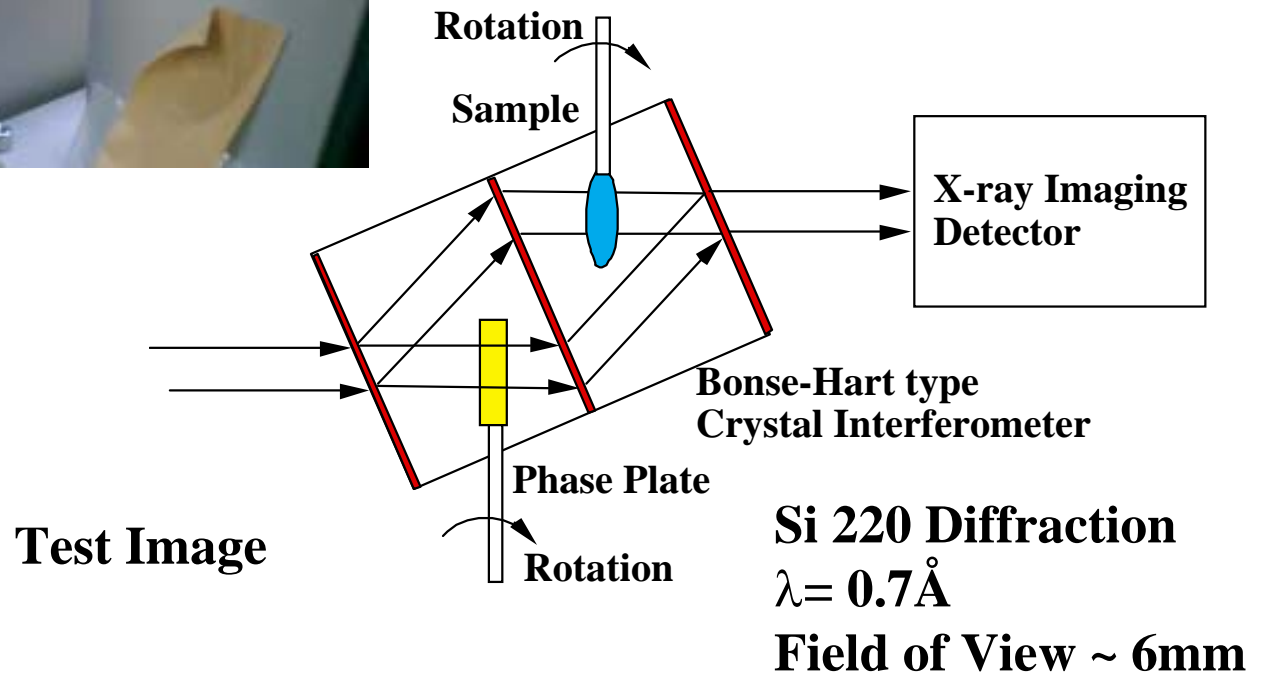
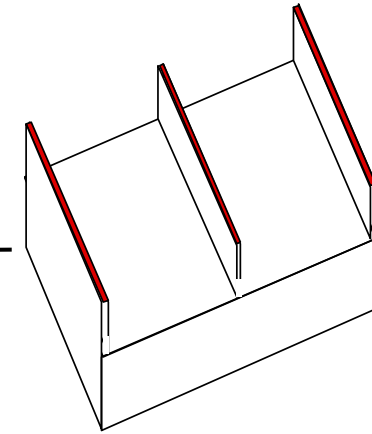
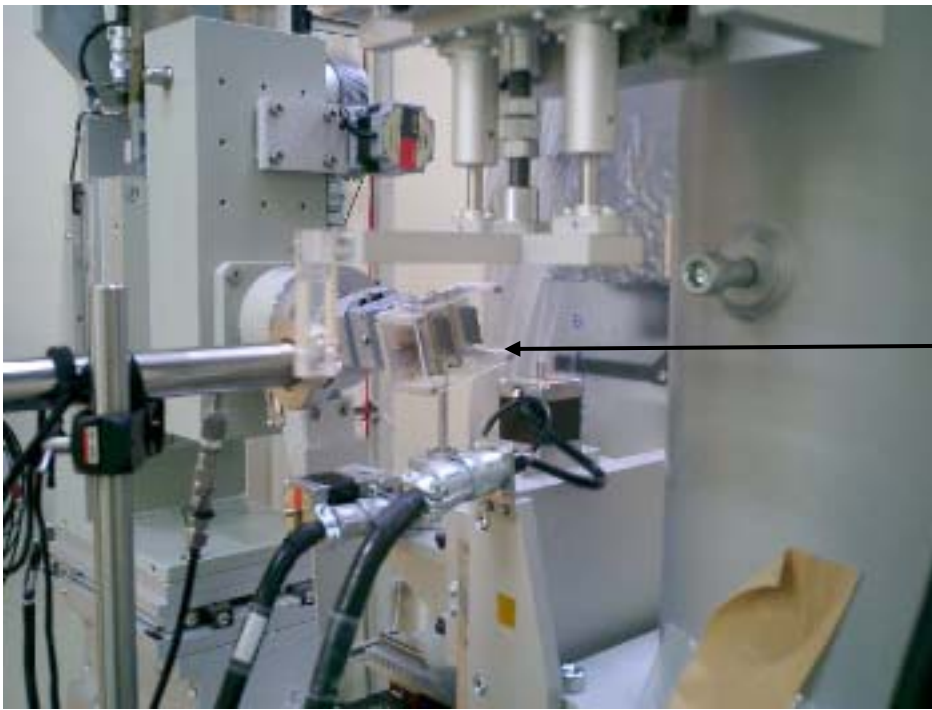


59 x 28 x 52  $\mu\text{m}$

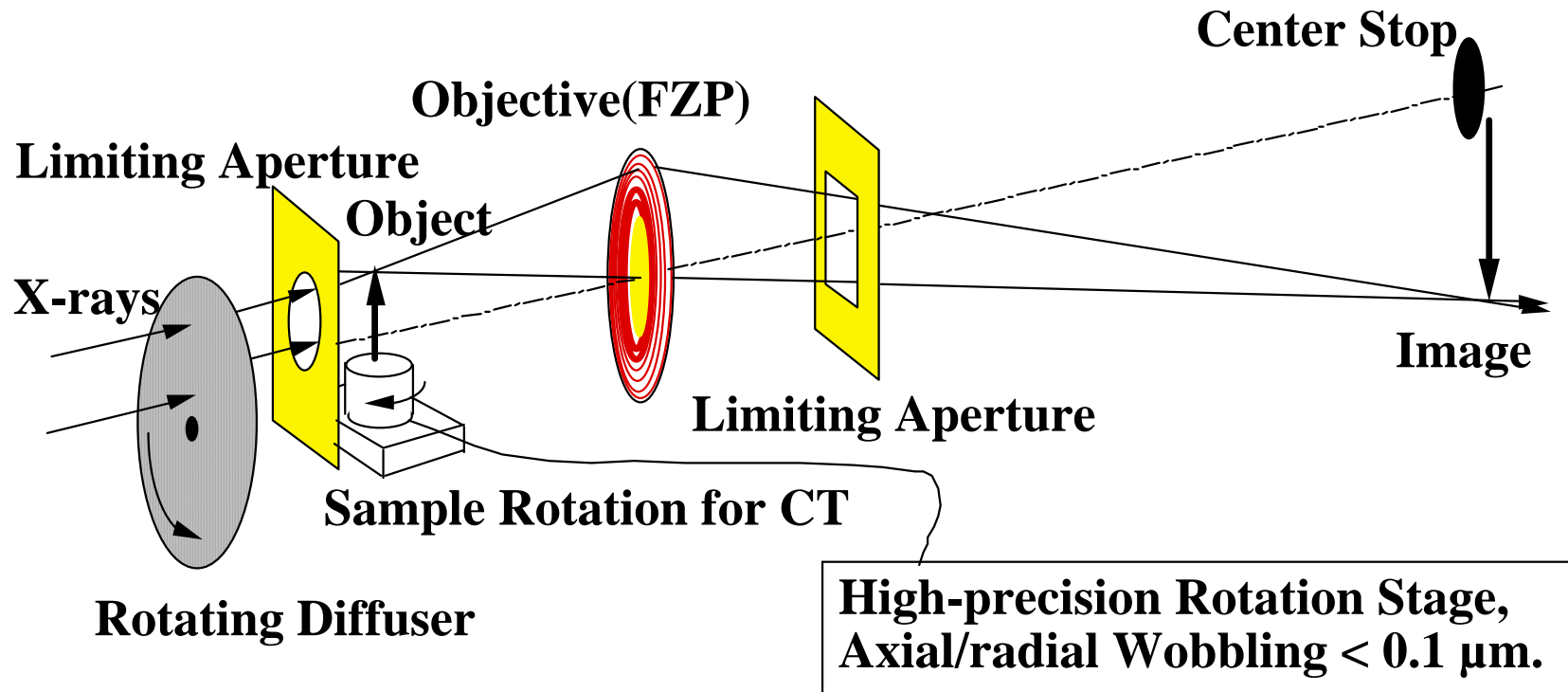
YAG phase is removed from 3D reconstructed image. Holes of the  $\text{Al}_2\text{O}_3$  phase indicates  $\text{Al}_2\text{O}_3$  and YAG phases are entangled each other. No holes are observed in conventional eutectic structures of metallic alloys.

Composition:  $\text{Al}_2\text{O}_3$ -18.5mol%  $\text{Y}_2\text{O}_3$   
Growth rate : 0.5mm/h

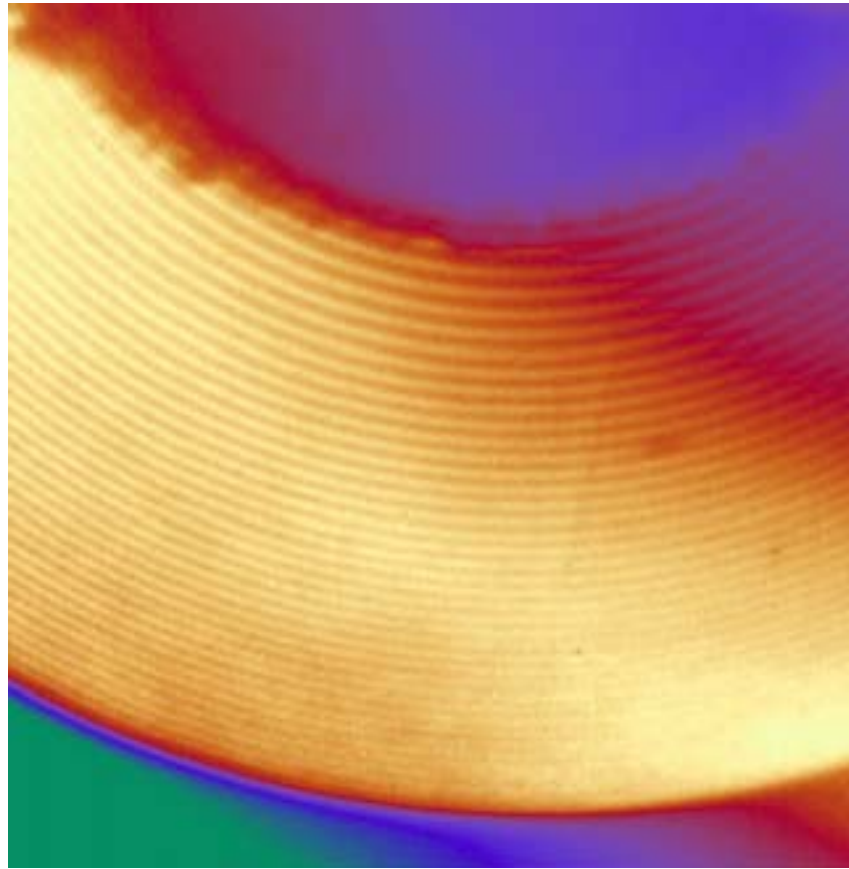
X-ray energy: 25keV  
Projection: 750 frames  
Resolution: 0.5 $\mu\text{m}$ /pixel



**Phase-contrast CT using Bonse-Hart Interferometer at BL20XU**

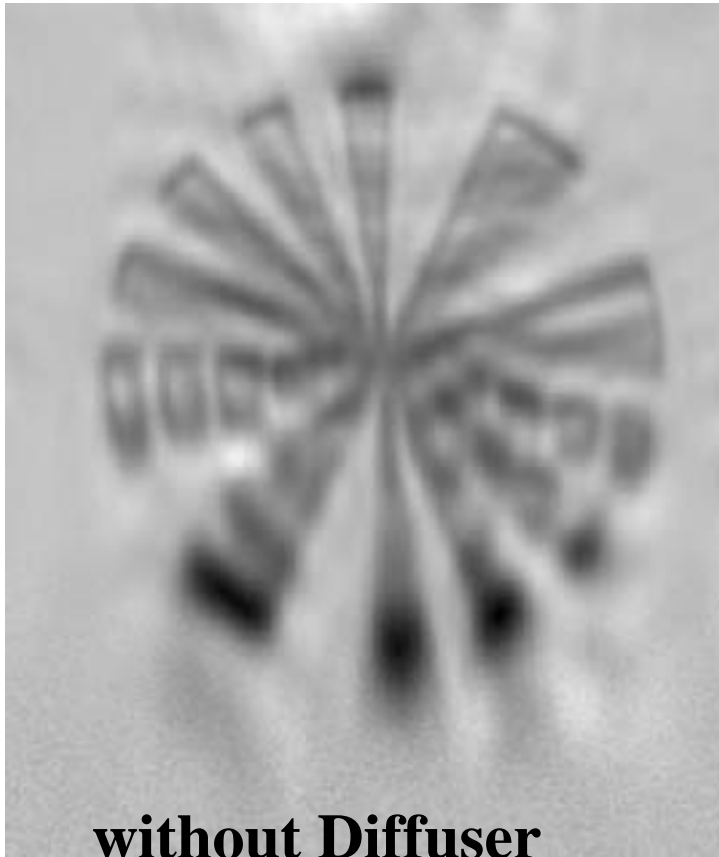


## Schematic Diagram Experimental Setup for Imaging Microscopy and Micro-tomography



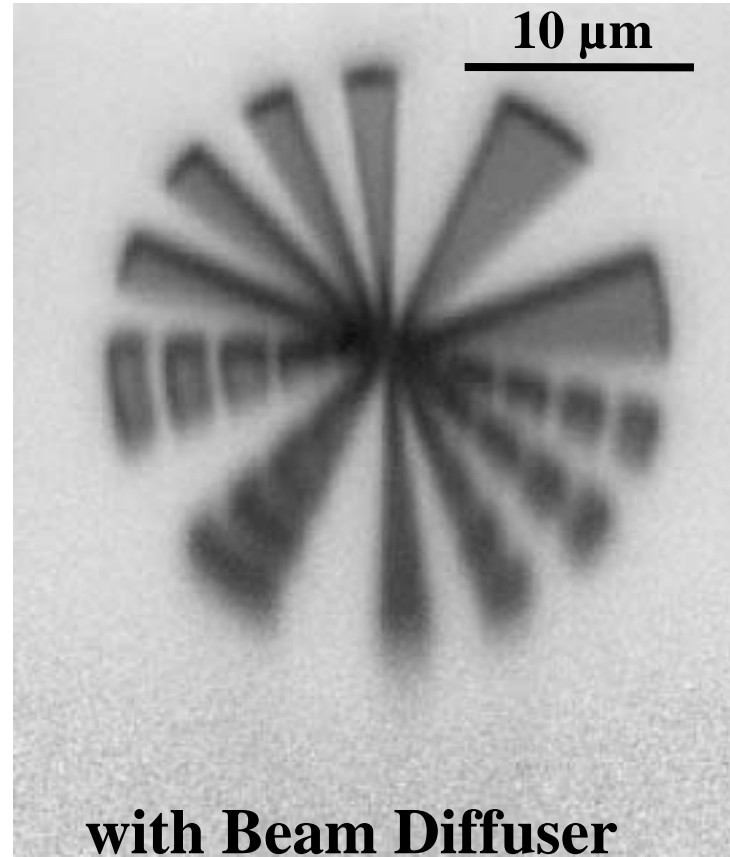
## **Imaging Microscopy**

**Objective & Sample: FZP with 0.25  $\mu\text{m}$  outermost zone width,  
X-ray Energy: 8 keV.**



**without Diffuser**

**- Coherent Illumination -**



**with Beam Diffuser**

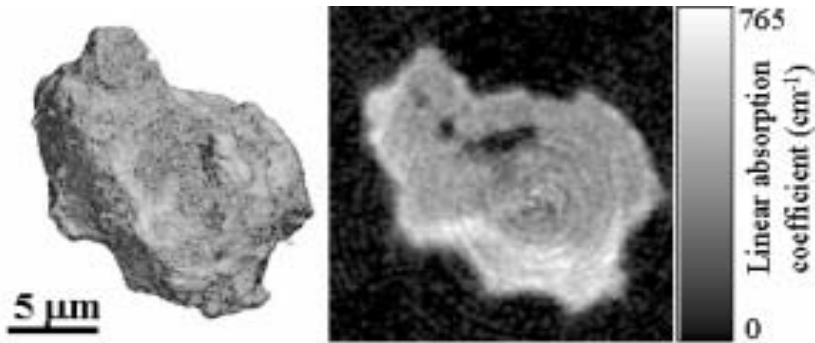
**- Incoherent Illumination-**

## **Imaging Microscopy with FZP Objective**

**- Effect of Beam Diffuser -**

**X-ray energy: 8 keV**

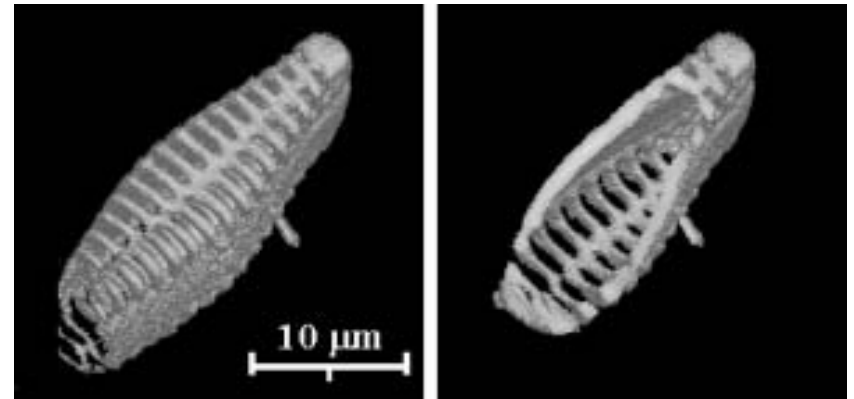
**Control of coherence is important!**



### **Stony Meteorite Allende**

**8 keV, x7.61, BM3(x10), voxel size 0.13 μm.**

**100 projection, exposure time:15 s/projection.**



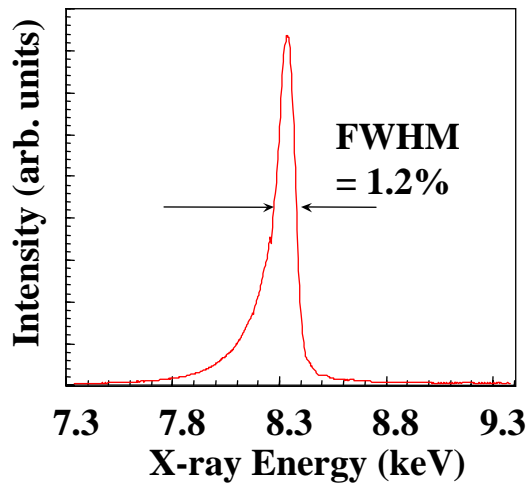
### **Diatom "Achnanthis lanceolata"**

**8 keV, x10, BM3(x10), voxel size 0.1 μm.**

**360 projection, exposure time: 60 s/projection.**

## **X-ray Micro-tomography using Imaging Optics with Fresnel Zone Plate Objective**

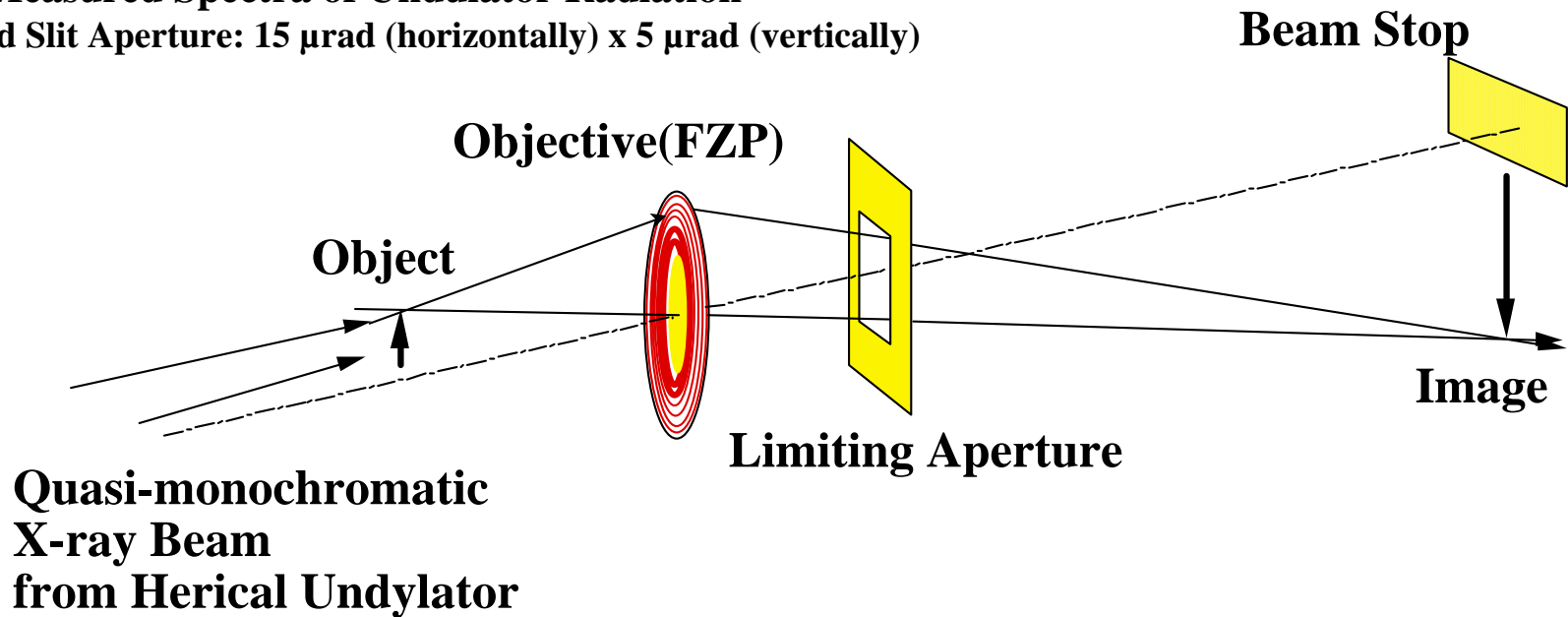




## Hard X-ray Imaging Microscopy with Fresnel Zone Plate Objective & Quasi-monochromatic Undulator Radiation

### Measured Spectra of Undulator Radiation

Front-end Slit Aperture:  $15\ \mu\text{rad}$  (horizontally)  $\times$   $5\ \mu\text{rad}$  (vertically)



## Experimental Setup at BL40XU SPring-8

## **BL40XU of SPring-8 (High Flux Beamline)**

- 1. Undulator radiation without monochromator,  $\Delta\lambda/\lambda \sim 1\%$ .**
- 2. Helical Undulator --> Suppression of higher order,**
- 3. Condenser Optics: K-B mirror**

**Available flux ~ 1000 times conventional beamlines  
(undulator beamlines with crystal monochromator).**

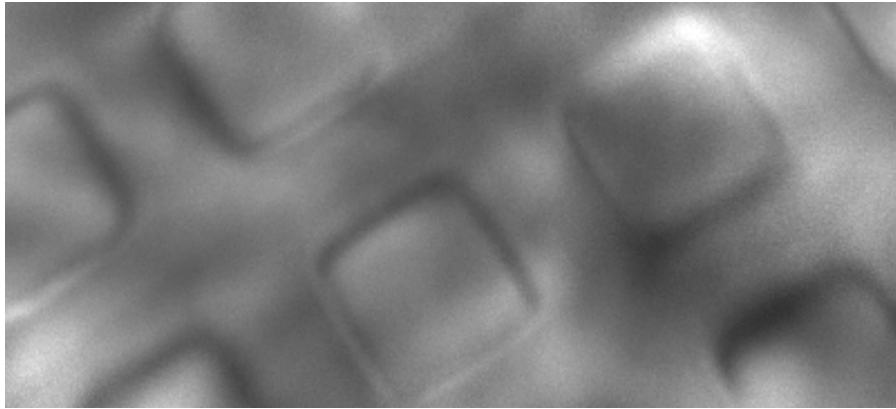
**Requirement on monochromaticity for Fresnel zone plate  
~ Number of Fresnel zone.**

**--->  $\Delta\lambda/\lambda \sim N$  (number of Fresnel zone)**

**Use of direct undulator radiation,  $\Delta\lambda/\lambda \sim 100$ .**

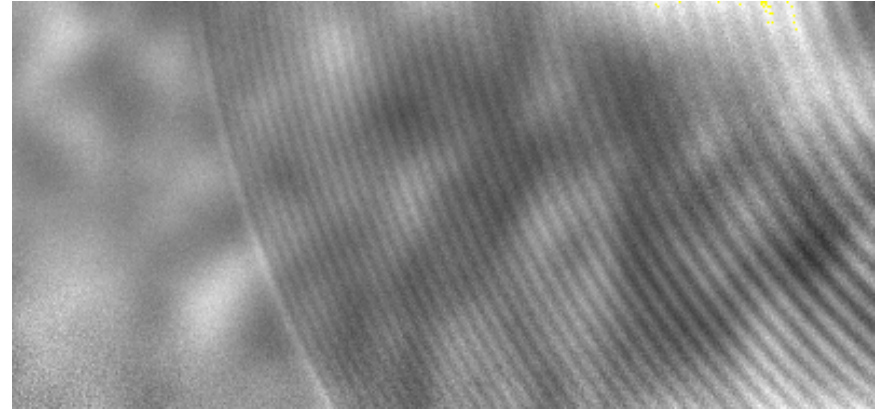
**X-ray imaging microscopy with sub- $\mu\text{m}$  resolution  
and milli-second exposure time!**

10  $\mu\text{m}$



**Object: Cu mesh,  
2000 lines/inch**

10  $\mu\text{m}$



**Object: Fresnel zone plate,  
0.25  $\mu\text{m}$  outermost zone width**

### **Image of test object**

**Objective: FZP, 0.25  $\mu\text{m}$  outermost zone width, 100 zones,**

**Magnification: 11.3,**

**X-ray energy: 8.34 keV,**

**Exposure time: 1.5 ms (Single Shot)**

**Hard X-ray Imaging Microscopy with Fresnel Zone Plate Objective  
& Quasi-monochromatic Undulator Radiation at BL40XU**

## **Summary and Future Project**

- 1. Microbeam, Scanning Microscopy, Imaging Microscopy  
submicron - 60 nm resolution in hard X-ray region.**
- 2. Micro-CT, XRF Analysis/imaging, topography, micro-diffraction.**

**~ 50% of general users @BL20B2 & 47XU is micro-CT,  
~ 80% of XRF users @BL37XU is microbeam analysis.**

**Wide varieties of spatial resolution and FoV(field of view) are required.  
Spatial resolution: 10  $\mu\text{m}$  - 100 nm, FoV: 100 mm -.  
Macroscopic -> intermediate -> microscopic -> nano-scopic!**

**Future,**

- 1. Spatial Resolution: 10 nm @4 - 100 keV.**
- 2. Variable field and spatial resolution are required for general use.**